Defect and Diffusion Forum Vol. 333 (2013) pp 51-60
Online available since 2013/Jan/25 at www.scientific.net

doi:10.4028/www.scientific.net/DDF.333.51

Diffusion Processes in Early Stages of Precipitation in Mg-Gd and Mg-Tb Alloys

Oksana Melikhova[1, a], Jakub Čížek[1,b], Petr Hruška[1,c], Martin Vlach[1,d], Bohumil Smola[1,e], Ivana Stulíková[1,f], Ivan Procházka[1,g]

[1]Faculty of Mathematics and Physics, Charles University, V Holešovičkách 2, CZ-180 00 Praha 8, Czech Republic

[a]oksana.melikhova@mff.cuni.cz, [b]jakub.cizek@mff.cuni.cz, [c]peta.hruska@gmail.com, [d]martin.vlach@mff.cuni.cz, [e]bohumil.smola@mff.cuni.cz, [f]ivana.stulikova@mff.cuni.cz, [g]ivan.prochazka@mff.cuni.cz

Keywords: Mg alloys, precipitation, natural aging, positron annihilation.

Abstract. Early stages of precipitation were investigated in solution treated binary Mg-Tb and Mg-Gd alloys. The supersaturated solid solution of Gd (or Tb) in Mg was formed by fast quenching of the alloys from solution treatment temperature. Decomposition of the supersaturated solid solution and precipitation effects were investigated by positron lifetime spectroscopy combined with microhardness testing. During solution treatment at elevated temperature some thermal vacancies form pairs with solute atoms. In quenched samples free vacancies are quickly annealed out, while more stable vacancies bound to solute atoms remain in the sample and enhance the diffusivity of solutes. The hardness of solution treated Mg-Tb and Mg-Gd alloys aged at ambient temperature rises due to formation of small clusters of Tb and Gd atoms. Isochronal annealing of Mg-Tb and Mg-Gd alloys leads to precipitation of coherent β'' phase, semicoherent β' phase and incoherent β phase particles. It was found that natural aging of Mg-Tb alloy at ambient temperature has beneficial effect on subsequent hardening by β'' phase particles formed during annealing.

Introduction

Lightweight hardenable Mg-alloys with rare earth alloying elements have taken considerable attention due to improved creep properties and good thermal stability of mechanical properties [1-4]. Binary Mg-Gd and Mg-Tb alloys are the base for novel creep resistant hardenable Mg alloys with rare earth elements [3,5,6]. The maximum solubility of Gd and Tb in Mg rapidly decreases with decreasing temperature [1]. Hence, supersaturated solid solution of Gd or Tb in Mg can be obtained by rapid quenching from elevated temperatures. With increasing temperature the supersaturated solid solution α' decomposes obeying the following sequences [2]:

Mg-Gd: α' (hcp) → β'' ($D0_{19}$) → β' (c-bco) → β (fcc, Mg_5Gd).

Mg-Tb: α' (hcp) → β'' ($D0_{19}$) → β' (c-bco and/or fcc) → β (bcc, $Mg_{24}Tb_5$).

Particles of the β'' transient phase with a hexagonal $D0_{19}$ structure are coherent with hexagonal close packed (hcp) Mg matrix and the β'' phase lattice parameters are related to those of Mg matrix as follows $a = 2a_{Mg}$, $c = c_{Mg}$. The β' transient phase exhibits *c*-base centered orthorhombic (c-bco) structure with lattice parameters $a = 2a_{Mg}$, $b \approx 8d(1\text{-}1\ 0\ 0)_{Mg}$ (i.e. eight times the distance between (1-1 0 0) planes in the Mg matrix), $c = c_{Mg}$. β' phase particles are semicoherent with the Mg matrix since coherency with Mg matrix is retained in the (01-10) plane only, while perpendicularly to this plane the coherency is lost. Particles of the stable β phase are completely incoherent with the Mg matrix. The lattice mismatch between particles of semicoherent or incoherent phase and Mg matrix is compensated by open-volume misfit defects. Hence, the formation of β' and β phase introduces

misfit defects into the sample. Precipitation of second phase particles is influenced by density of nucleation centers and also by the diffusivity of solute elements. The latter is facilitated by quenched-in vacancies bound to solute atoms [7]. Hence, vacancies frozen in the alloy quenched from solution treatment temperature play a very important role in precipitation effects.

The present work is focused on early stages of precipitation in Mg-Tb and Mg-Gd alloys and on the role of vacancies in these processes. Characterization of quenched-in vacancies and open volume misfit defects at the interfaces between second phase precipitates and Mg matrix was performed by two complementary techniques of positron annihilation: (i) positron lifetime (LT) spectroscopy [8] and (ii) coincidence Doppler broadening (CDB) [9]. LT spectroscopy enables identification of defects in the sample and determination of defect densities, while CDB carries information about the local chemical environment of defects. Combination of LT and CDB spectroscopy represents a valuable tool for investigation of precipitation effects in Mg-alloys [10-14].

Experimental

Samples. Binary Mg-13.39wt.%Tb (Mg13Tb) and Mg-14.58wt.%Gd (Mg15Gd) alloys were produced by squeeze casting under a protective gas atmosphere (Ar + 1%SF_6). Results of chemical analysis of both alloys are given in Table 1. The as-cast Mg13Tb and Mg15Gd alloys were solution treated for 6 h at 530^{o}C and 500^{o}C, respectively. The solution treatment was performed in a vertical furnace with protective Ar atmosphere and was finished by quenching into water at room temperature.

In order to monitor dissolution of Tb and Gd in the Mg matrix during the solution treatment additional specimens of both alloys were solution treated for various times and examined by measurement of Vickers microhardness (HV). Development of HV in Mg13Tb and Mg15Gd alloy solution treated for various times is shown in Fig. 1(a) and 1(b), respectively. Solution treatment causes a decrease of HV due to gradual dissolution of Gd and Tb in Mg matrix. Finally HV approaches a plateau value indicating that all alloying elements were dissolved in the Mg matrix. From inspection of the Figure one can conclude that solution treatment for 6 h is sufficient for a complete dissolution of Gd and Tb in the Mg matrix in both alloys.

After characterization of solution-treated samples the alloys were subjected to step-by-step isochronal annealing with the effective heating rate 1 K/min. Each annealing step was finished by quenching into water of room temperature.

Table 1 Chemical composition (in wt.%) of Mg13Tb and Mg15Gd alloy. Concentration of other impurities not shown in the Table is less than 0.01 wt.%

	Tb	Gd	Y	Dy	Mn	Fe	Al	Cu	Mg
Mg13Tb	13.39	0.05	0.10	0.10	0.02	0.03	0.01	0.01	balance
Mg15Gd	0.01	14.58	0.05	0.01	0.01	0.02	0.02	0.02	balance

Methods of characterization. A carrier-free $^{22}Na_2CO_3$ positron source with activity of ≈ 1 MBq deposited on 2 μm thick mylar foil was used for investigations by positron annihilation spectroscopy. The positron source always formed a sandwich with two pieces of studied sample.

A digital positron lifetime spectrometer described in Ref. [15] was employed for LT studies. The spectrometer exhibits excellent time resolution of 145 ps (full width at half maximum of the resolution function for ^{22}Na positron source). At least 10^7 annihilation events were accumulated in each LT spectrum. The source contribution which comes from positrons annihilated in the $^{22}Na_2CO_3$ spot and the covering mylar foil consists of two weak components with lifetimes of 0.368 and 1.5 ns and relative intensities of 8% and 1% and was determined using a well annealed reference pure Mg (99.99%) sample.

CDB measurements were carried out using a digital spectrometer [16] equipped with two coaxial HPGe detectors. Total resolution of our CDB spectrometer is 1.00 keV. The total statistics accumulated in each two-dimensional CDB spectrum was at least 10^8 positron annihilation events. Two dimensional CDB spectra were subsequently reduced into one-dimensional cuts representing Doppler-broadened annihilation profile and resolution function of the spectrometer [9,16]. CDB results in this work are presented as ratio curves related to a well annealed pure Mg (99.99%) reference. In addition pure Gd (99.9%) and Tb(99.9%) reference samples were examined by CDB in order to obtain shape of the electron momentum distribution in these two materials.

Both LT and CDB measurements were performed at room temperature. It takes typically ~ 2 days to accumulate a single LT or CDB spectrum with sufficient statistics.

A Struers Duramin 300 hardness tester was employed for HV measurements by Vicker's technique using a load of 100 g applied for 10 s.

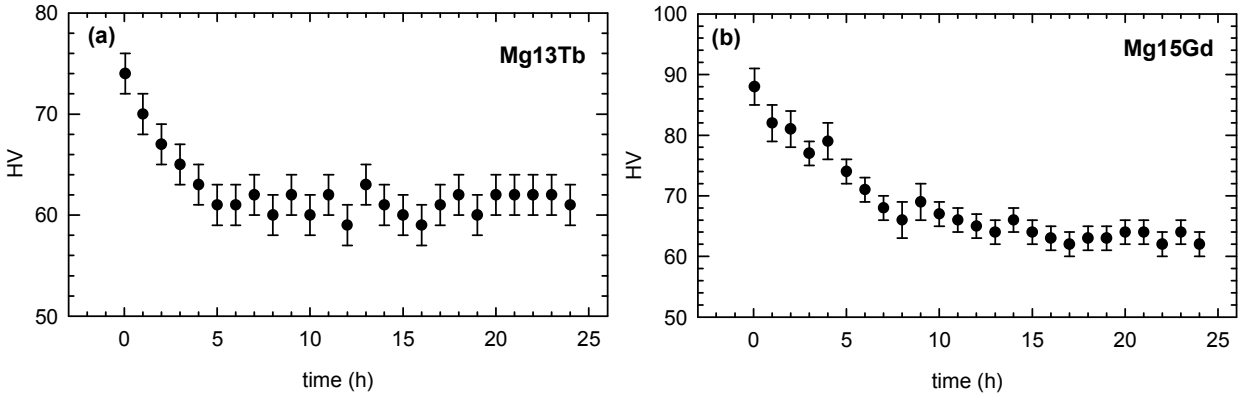

Figure 1 Development of microhardness HV during solution treatment: (a) Mg13Tb alloy solution treated at 530°C, (b) Mg15Gd solution treated at 500°C.

Results

Solution treated alloys. Positron lifetimes τ_i and relative intensities I_i of the exponential components resolved in LT spectra of solution treated samples are listed in Table 2. Both Mg13Tb and Mg15Gd alloy measured immediately after quenching exhibit a two-component LT spectrum. The short-lived component with lifetime τ_1 represents a contribution of free positrons not trapped at defects, while the long-lived component with lifetime τ_2 comes from positrons trapped at quenched-in vacancies. Indeed, the lifetime τ_2 of the latter component is close to the calculated lifetime for a vacancy in Mg [17].

In Mg alloys an attractive interaction likely exists between vacancies and Gd or Tb solutes having a larger size than Mg atoms. Positive correlation between the solute – vacancy binding energy and the solute size is well documented for dilute Al alloys [18,19]. A large impurity atom placed into the matrix imposes a significant strain on the surrounding atoms. A vacancy located next to this large impurity atom allows the impurity to relax to the open volume in the vacancy. Such inward relaxation of the impurity towards the vacancy releases the strain imposed on the neighboring atoms and causes an energy decrease [18]. Hence, by analogy with Al alloys one can expect that complexes of vacancies bound with Gd or Tb atoms are formed also in Mg-alloys during solution treatment at elevated temperature. Single vacancies in Mg are mobile well below room temperature and in quenched sample quickly disappear by diffusion to sinks at the surface and grain boundaries [20]. However, vacancy-solute pairs are more stable and may remain in the alloys quenched to room temperature. Hence, the component with lifetime τ_2 detected in quenched Mg13Tb and Mg15Gd samples can be attributed to positrons trapped at vacancies bound to Gd or Tb atoms.

Table 2 Results of LT measurements of solution treated alloys: lifetimes τ_i and relative intensities I_i of the components resolved in LT spectra for solution treated alloys measured immediately after quenching (quenched) and after aging at ambient temperature for various time periods (aged). The concentration of quenched-in vacancies c_v calculated using Eq. (1) is given in the last column.

sample	state	τ_1 (ps)	I_1 (%)	τ_2 (ps)	I_2 (%)	c_v (ppm)
Mg13Tb	quenched	214.0(8)	84.3(7)	280(15)	15.7(7)	16(1)
	aged 4 days	215.1(8)	85.0(5)	290(10)	15.0(5)	16(1)
	aged 2 months	225.5(2)	100	-	-	< 1
Mg15Gd	quenched	214.6(7)	80.5(7)	295(5)	19.5(6)	23(2)
	aged 4 days	215.0(8)	81.2(6)	290(10)	18.8(6)	21(2)
	aged 2 months	225.4(2)	100	-	-	< 1

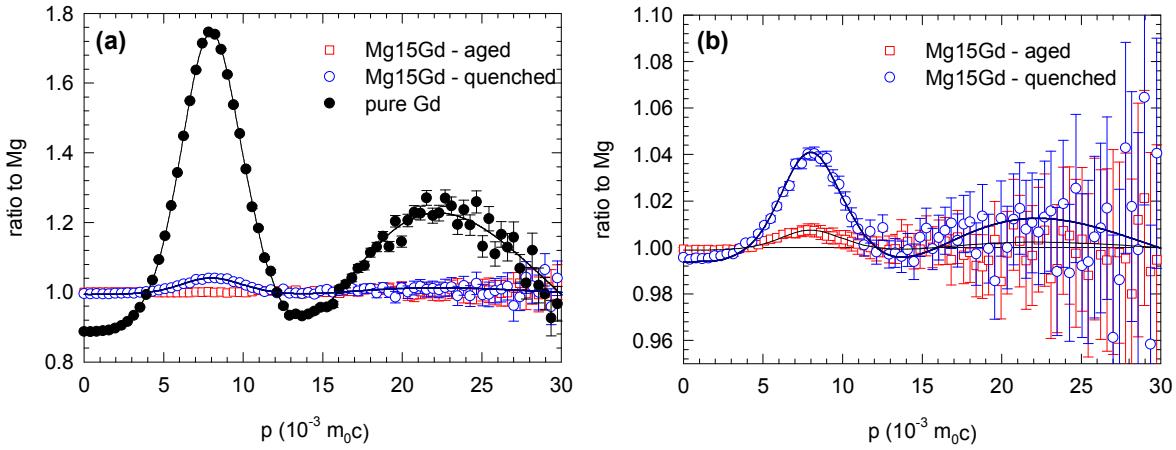

Figure 2 (a) CDB ratio curves (related to annealed pure Mg) for Mg15Gd alloy measured immediately after quenching (open circles) and after natural aging for 2 months (open squares). Ratio curve for a pure Gd (99.9%) reference is plotted by full points; (b) A detail of CDB ratio curves (related to annealed pure Mg) for Mg15Gd alloy measured immediately after quenching and after natural aging for 2 years. Solid lines which describe well the experimental points for the quenched and the aged alloy show the pure Gd contribution rescaled to 5 and 2.5%, respectively.

Formation of complexes of vacancies bound to Gd or Tb solutes was confirmed by detailed CDB investigations of as-quenched alloys. CDB ratio curves (related to pure Mg) for Mg15Gd alloy and pure Gd (99.9%) reference are plotted in Fig. 2(a). The curve for Gd exhibits a sharp peak at the momentum $p \approx 8 \times 10^{-3}$ m_0c followed by a broader peak at $p \approx 23 \times 10^{-3}$ m_0c. The curve for Mg15Gd measured immediately after quenching exhibits similar peaks which testifies to a contribution of positrons annihilated by Gd electrons. Fig. 2(b) shows that the curve for quenched Mg15Gd is well described by a 5% contribution of positrons annihilated by Gd electrons which is comparable with the fraction of positrons trapped in vacancies estimated from LT data using the simple trapping model [8]. Hence, positrons trapped at quenched-in vacancies are annihilated predominantly by Gd electrons.

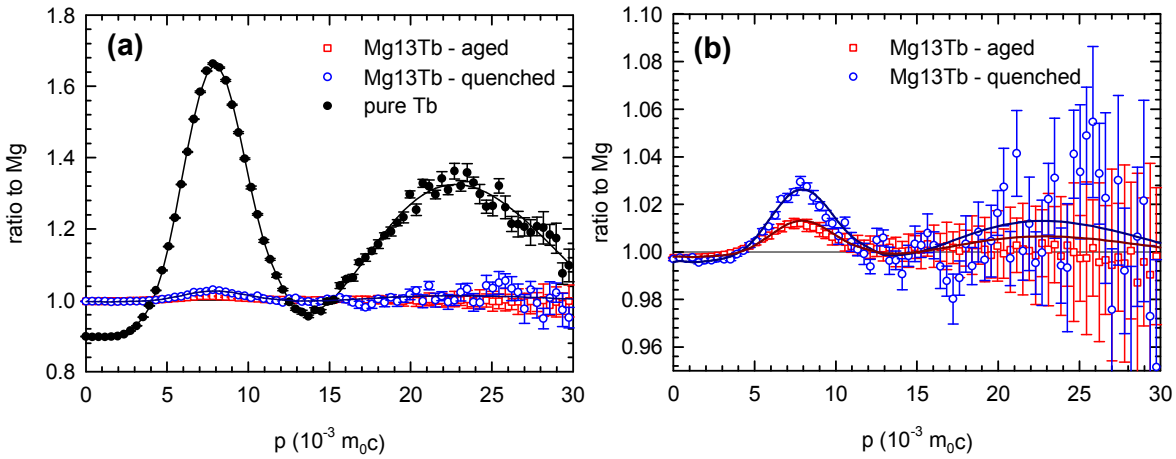

Figure 3 (a) CDB ratio curves (related to annealed pure Mg) for Mg13Tb alloy measured immediately after quenching (open circles) and after natural aging for 2 months (open squares). Ratio curve for a pure Tb (99.9%) reference is plotted by full points; (b) A detail of CDB ratio curves (related to annealed pure Mg) for Mg13Tb alloy measured immediately after quenching and after natural aging for 2 years. Solid lines show the pure Tb contribution rescaled to 4 and 2.2%. These curves describe well the experimental points for the quenched and the aged Mg13Tb alloy.

In Fig. 3(a) the CDB ratio curves for Mg13Tb alloy are compared with the ratio curve for a pure Tb (99.9%) reference. The ratio curves for pure Tb and Gd are similar, i.e. similarly to Gd the ratio curve for pure Tb exhibits a sharp peak at the momentum $p \approx 8 \times 10^{-3}$ m_0c followed by a broader peak at $p \approx 23 \times 10^{-3}$ m_0c. From comparison of Figs. 2(a) and 3(a) one can realize that the latter peak is more pronounced in Tb than in Gd. Fig. 3(b) shows a detail view of the ratio curves for Mg13Tb alloy in the as-quenched state and after ageing for 2 months. Obviously the ratio curves for Mg13Tb alloy exhibit features similar to those in the curve for pure Tb. This is demonstrated by solid lines in Fig. 3(b) which describes well the experimental points. The ratio curve for as-quenched Mg13Tb alloy is well described by 4% contribution of positrons annihilated by Tb electrons. This is again comparable with the fraction of positrons trapped at vacancies testifying, therefore, that vacancies in quenched Mg13Tb alloy are associated with Tb atoms.

The concentration c_v of quenched-in vacancies associated with Tb or Gd atoms can be calculated from LT data using the simple trapping model [8]

$$c_v = \frac{1}{\nu_V} I_2 \left(\frac{1}{\tau_1} - \frac{1}{\tau_2} \right), \qquad (1)$$

where $\nu_v = 1.1 \times 10^{13}$ s^{-1} is the specific positron trapping rate for a vacancy in Mg [21]. The concentrations of quenched-in vacancies calculated from Eq. (1) are given in the last column in Table 2.

LT studies were performed not only for quenched alloys but also for alloys naturally aged for various time periods, see arrows in Fig. 2. One can see in Table 2 that the sample naturally aged for 4 days (96 h) contains quenched-in vacancies in concentration comparable to that in the quenched sample. Hence, quenched-in vacancies remaining in the samples facilitate diffusion and clustering of solutes. However, after natural aging for 2 months the solute clusters are fully developed and bound vacancies are removed from the samples, which leads to the disappearance of the component with the lifetime τ_2, see Table 2.

Disappearance of vacancies in alloys aged for 2 months is reflected also by a drop of the CDB contribution of positrons annihilated by Gd or Tb electrons down to ≈ 2.5 %, see Figs. 2(b) and 3(b). This value is comparable with the atomic concentration of Gd and Tb solutes which is 2.7 at.% in Mg15Gd and 2.2 at.% in Mg13Tb. In the alloys aged for 2 months positrons annihilate from the

free state, see Table 2. Free positron delocalized in the lattice can still by chance be annihilated by a Gd or Tb electron. But the probability that it happens is comparable with the atomic concentration of Gd or Tb atoms and is significantly lower than that for a positron trapped at vacancies associated with solute atoms.

Fig. 4 shows development of HV for solution treated Mg13Tb and Mg15Gd alloy left at ambient temperature after quenching. Obviously in both alloys HV rises significantly with increasing aging period at ambient temperature. Enhanced HV in both alloys is achieved by aging at ambient temperature for ~ 600 h. Fig. 4 shows also development of HV for solution treated alloys kept at liquid nitrogen temperature (-196°C). Contrary to alloys aged at ambient temperature, alloys stored in liquid nitrogen do not show any increase of HV. This testifies that natural aging occurring in Mg13Tb and Mg15Gd is a thermally activated process. Since the solubility of Tb and Gd in Mg strongly decreases with decreasing temperature small clusters of Tb or Gd atoms are formed during aging at ambient temperature by diffusion of Gd or Tb alloying elements. Driving force for the clustering of Tb and Gd atoms is solute supersaturation in the Mg matrix. Clustering process is obviously controlled by temperature and is facilitated by quenched-in vacancies bound to solute atoms

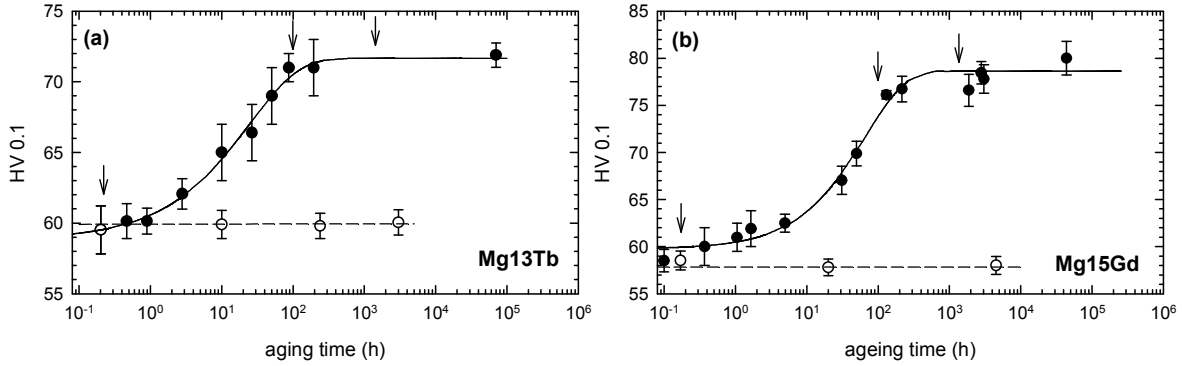

Figure 4 Development of HV of solution treated alloys during natural aging at ambient temperature (full points). For comparison development of HV in alloys stored at liquid nitrogen temperature is plotted in the figure as well (open points). Arrows indicate states measured by LT spectroscopy.

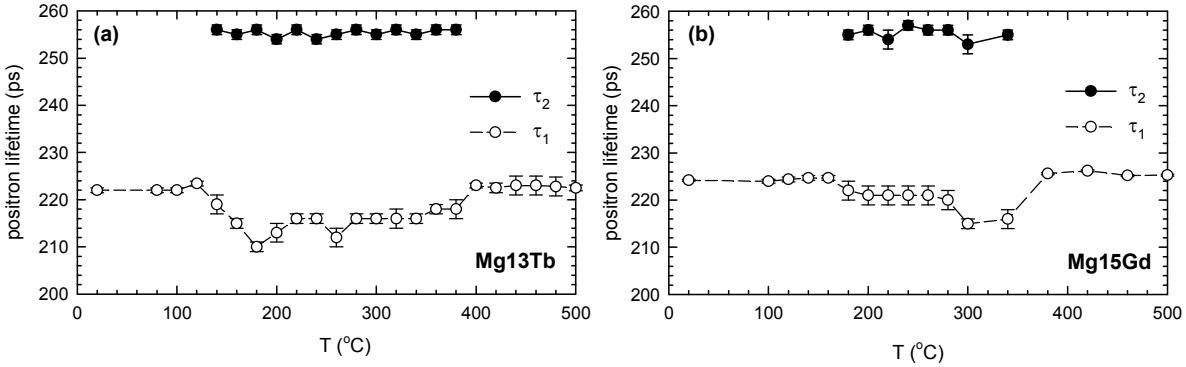

Figure 5 Temperature dependences of the lifetimes of exponential components resolved in LT spectra measured in (a) Mg13Tb and (b) Mg15Gd alloy aged for 2 months and then subjected to isochronal annealing. Open points: lifetime of free positrons; full points: lifetime of positrons trapped at vacancy-like defects.

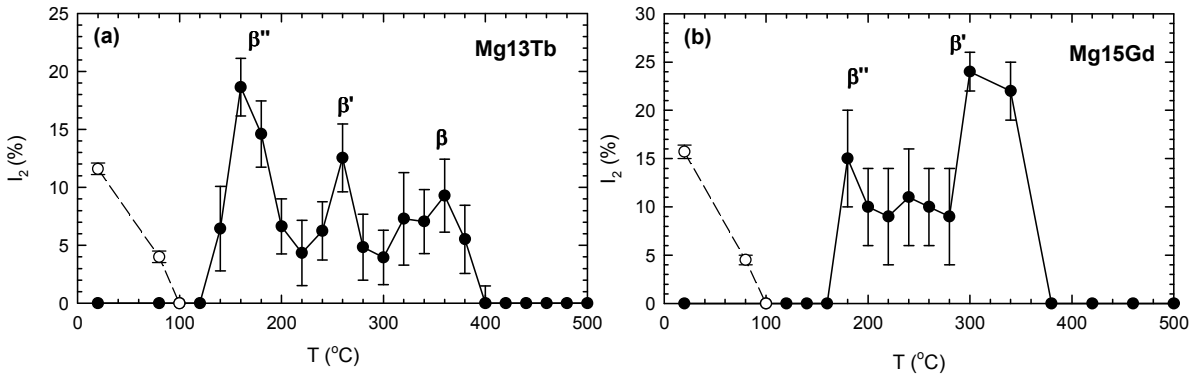

Figure 6 Temperature dependence of the relative intensity I_2 of positrons trapped at vacancy-like defects in (a) Mg13Tb and (b) Mg15Gd alloy aged for 2 months and then subjected to isochronal annealing. Full points show results for alloys naturally aged for 2 months, while open points show recovery of quenched-in vacancies in alloys annealed immediately after quenching.

Isochronal annealing. Solution treated alloys aged at ambient temperature for ~2 months were subjected to step-by-step isochronal annealing with effective heating rate of 1 K/min. Development of microstructure after each annealing step was investigated by LT spectroscopy and HV testing. Temperature dependences of lifetimes of the exponential components resolved in LT spectra for Mg13Tb and Mg15Gd alloy are plotted in Fig. 5(a) and 5(b), respectively. The relative intensity I_2 of the component originating from positrons trapped at vacancy-like defects in Mg13Tb and Mg15Gd alloy is plotted in Fig. 6(a) and 6(b), respectively. From inspection of Figs. 5, 6 one can conclude that Mg13Tb and Mg15Gd alloys isochronally annealed up to 120°C and 160°C, respectively, exhibit a single component spectrum with lifetime $\tau_1 \approx 225$ ps corresponding to free positrons annihilated in Mg matrix. In alloys annealed to higher temperatures precipitates of second phase particles are formed which is reflected by appearance of additional component with lifetime $\tau_2 \approx 255$ ps and relative intensity I_2. Lifetime of this component is comparable with vacancy-like defects associated with dislocations in Mg or misfit defects and precipitate-matrix interfaces [10]. Hence, formation of second phase precipitates introduces vacancy-like defects into Mg13Tb and Mg15Gd alloy. Indeed, semicoherent β' particles and incoherent β precipitates contain vacancy like misfit defects at interfaces between the precipitates and the Mg matrix. Particles of β'' phase are coherent with the Mg matrix and, thereby, do not exhibit misfit defects at the interfaces. However, the structure of β'' phase particles contains most probably vacancies in the equivalent sites for Gd or Tb atoms. The concentration of vacancy-like defects calculated using Eq. (1) is plotted in Fig. 7. Obviously precipitation of the second phase particles causes a rise of the concentration of vacancy-like defects c_v, while coarsening and dissolution of these particles leads to a decrease of c_v. Precipitation of β'', β' and β phase can be distinguished in Mg13Tb in Fig. 7(a). In Mg15Gd (Fig. 7(b)) the first peak corresponds to the β'' and the second peak at 300°C is most probably connected with the β' phase. Formation of the β'' phase with $D0_{19}$ structure was detected in the temperature range 140-180°C and 160-200°C in Mg13Tb and Mg15Gd, respectively. This is in agreement with TEM observations, which revealed diffusion spots from ordered $D0_{19}$ phase in Mg13Tb [22] and Mg15Gd [23] isochronally annealed up to 180 and 200°C, respectively.

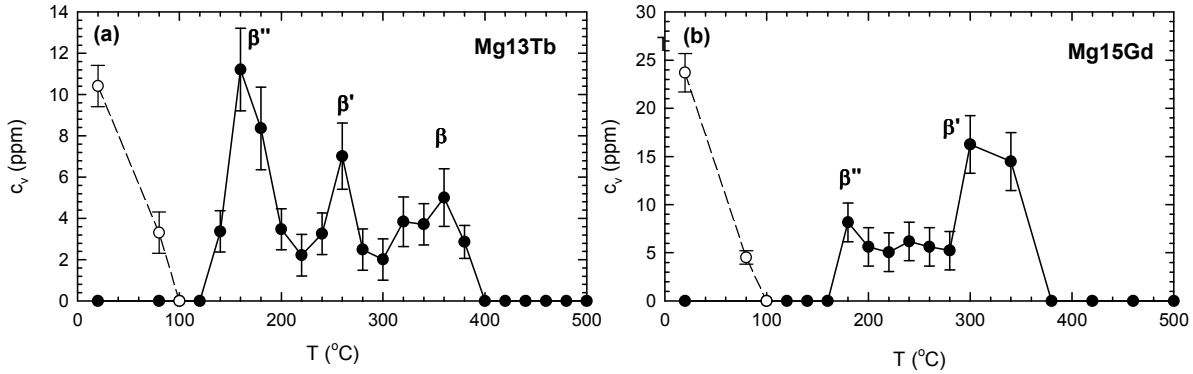

Figure 7 The concentration of vacancy-like defects determined by LT spectroscopy in (a) Mg13Tb and (b) Mg15Gd alloy subjected to isochronal annealing. Full points show results for alloys naturally aged for 2 months. Recovery of quenched-in vacancies in alloys annealed immediately after quenching is shown by open points.

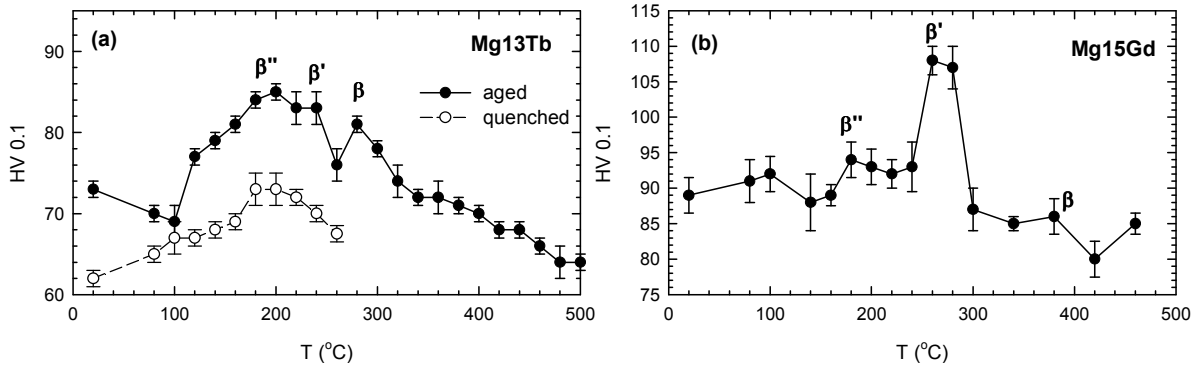

Figure 8 Development of HV in (a) Mg13Tb, (b) Mg15Gd alloy subjected to isochronal annealing. Full points show results for alloy aged at ambient temperature for 2 months. Development of HV in Mg13Tb alloy isochronally annealed immediately after quenching is plotted in the left panel by open points.

In alloys aged at room temperature for 2 months clusters of solute Tb and Gd atoms developed and quenched-in vacancies disappeared. To characterize thermal stability of quenched-in vacancies bound to solutes another set of solution treated samples of both alloys was investigated. The samples were subjected to isochronal annealing immediately after quenching, i.e. without any ageing at ambient temperature. Open points in Fig. 7 show temperature dependence of the concentration of quenched-in vacancies calculated by Eq. (1) for the alloys isochronally annealed immediately after quenching. One can see in the Figure that quenched-in vacancies bound to solutes are removed by annealing up to 100°C in both alloys.

Development of HV during isochronal annealing of alloys aged after solution treatment at ambient temperature for 2 months is plotted in Fig. 8 by full points. In Mg13Tb alloy HV rises due to formation of β'' phase particles and maximum hardening is achieved at 200°C. Additional hardening peak appearing at 280°C is caused most probably by precipitation of the stable β phase. A rise of HV is observed at 180°C in Mg15Gd alloy when precipitation of coherent particles of β" phase takes place. Peak hardening in Mg15Gd alloy occurs at 270°C due formation to semicoherent particles of β' phase.

Open points in Fig. 8(a) show temperature dependence of HV in Mg13Tb sample which was isochronally annealed immediately after quenching, i.e. prior to development of Tb clusters. Lower initial HV of this sample is, therefore, caused by the fact that Tb clusters have not been developed yet. Obviously hardening in the sample annealed immediately after quenching is lower compared to

that in the aged sample. Thus, natural aging has beneficial affect on hardening in Mg13Tb alloy. This is likely due to the fact that small Tb clusters formed during natural aging serve as nucleation centers for β'' phase and enable formation of finely dispersed β'' particles.

Summary

Precipitation effects in Mg13Tb and Mg15Gd alloy were characterized by LT and CDB spectroscopy combined with HV testing. The solution treated alloys contain quenched-in vacancies bound to Tb or Gd solute atoms. Quenched-in vacancies facilitate diffusion of solute atoms and formation of small Tb or Gd clusters during aging at ambient temperature. Formation of the solute clusters at ambient temperature causes an increase of hardness. Precipitation of second phase particles in the samples subjected to isochronal annealing introduces vacancy-like defects and causes further hardening. The peak hardening in Mg13Tb alloy is caused by finely dispersed coherent β'' phase particles, while the maximum HV in Mg15Gd alloy is achieved by formation of semicoherent β' phase precipitates. It was found that natural aging at ambient temperature has a beneficial effect on hardening of Mg13Tb alloy during annealing.

Acknowledgement

This work was supported by the Czech Science Foundation (project P108/10/0648).

References

[1] L.L. Rokhlin: Magnesium Alloys Containing Rare Earth Metals, Taylor and Francis, London (2003)

[2] G.W. Lorimer: Proc. of the London Conference Mg Technology, London (1986), p. 47

[3] B.L. Mordike: Mat. Sci. Eng. A Vol. 324 (2002), p. 103

[4] P. Vostrý, I. Stulíková, B. Smola, M. Cieslar and B.L. Mordike: Z. Metallkde Vol. 79 (1988), p. 340

[5] B.L. Mordike and T. Ebert: Mater. Sci. Eng. A Vol. 302 (2001), p. 37

[6] I. A. Anyanwu, Y Kitaguchi, I. Harima, S. Kamado, Y. Kojima, S. Tanike and I. Seki, in: *Magnesium 97*, edited by E. Agion, D. Eliezer, Magnesium research institute (MRI) Ltd., Beer-Sheva, (1997), p.127

[7] J. Čížek, O. Melikhova, I. Procházka, J. Kuriplach, I. Stulíková, P. Vostrý and J. Faltus: Phys. Rev. B Vol. 71 (2005), 064106

[8] P. Hautojärvi and C. Corbel, in: *Proc. International School of Physics "Enrico Fermi", Course CXXV*, edited by A. Dupasquier, A.P. Mills, IOS Press, Varena (1995), p. 491

[9] P. Asoka-Kumar, M. Alatalo, V.J. Ghosh, A.C. Kruseman, B. Nielsen, K.G. Lynn: Phys. Rev. Lett. Vol. 77 (1996), p. 2097

[10] J. Čížek, I. Procházka, B. Smola, I. Stulíková, M. Vlach, V. Očenášek, O.B. Kulyasova and R.K. Islamgaliev: Int. J. Mat. Res. Vol. 100 (2009), p. 780

[11] R. Ferragut, F. Moia, F. Fiori, D. Lussana and G. Riontino: J. Alloys Compd. Vol. 495 (2010), p. 408

[12] B. Smola, I. Stulíková, J. Černá, J. Čížek and M. Vlach: Phys. Status Solidi A Vol. 208, (2011), p. 2741

[13] O. Melikhova, J. Čížek, P. Hruška, M. Vlček, I. Procházka, M. Vlach, I. Stulíková, B. Smola, N. Žaludová, R.K. Islamgaliev: Defect and Diffusion Forum Vol. 322 (2012), p. 151

[14] J. Čížek, M. Vlček, B. Smola, I. Stulíková, I. Procházka, R. Kužel, A. Jäger, P. Lejček: Scripta Mater. Vol. 66, (2012), p. 630

[15] F. Bečvář, J. Čížek, I. Procházka and J. Janotová: J. Nucl. Instrum. Methods A Vol. 539 (2005), p. 372

[16] J. Čížek. M. Vlček, I. Procházka: Nucl. Instrum. Methods A 623, 982 (2010).

[17] J. M. Campillo Robles, E. Ogando and F. Plazaola: J. Phys.: Condens Matter Vol. 19 (2007), 176222

[18] C. Wolverton: Acta Mater. 55, 5867 (2007).

[19] M. Ohta, F. Hashimoto: J. Phys. Soc. Jpn. 19, 1987 (1964).

[20] P. Tzanetakis, J. Hillairet and G. Revel: Phys. Stat. Sol. (b) Vol. 75 (1976), p. 433

[21] G.M. Hood: Phys. Rev. B Vol. 26 (1982), p. 1036

[22] J. Čížek, B. Smola, I. Stulíková, P. Hruška, M. Vlach, M. Vlček, O. Melikhova and I. Procházka: Phys. Stat. Sol. A (2012) in print doi: 10.1002/pssa.201228327

[23] P. Vostrý, B. Smola, I. Stulíková, F. von Buch and B.L. Mordike: Phys. Stat. Sol. (a) Vol. 175 (1999), p. 491

Recent Advances in Mass Transport in Engineering Materials
10.4028/www.scientific.net/DDF.333

Diffusion Processes in Early Stages of Precipitation in Mg-Gd and Mg-Tb Alloys
10.4028/www.scientific.net/DDF.333.51